Microfluid Nanofluid
DOI 10.1007/s10404-012-1066-8

RESEARCH PAPER

Rapid prototyping of glass-based microfluidic chips utilizing two-pass defocused CO_2 laser beam method

Lung-Ming Fu · Wei-Jhong Ju · Ruey-Jen Yang · Yao-Nan Wang

Received: 23 June 2012 / Accepted: 13 September 2012

Abstract A method is proposed for the scribing of glass substrates utilizing a commercial CO_2 laser system. In the proposed approach, the substrate is placed on a hotplate and the microchannel is then ablated using two passes of a defocused laser beam. The aspect ratio and surface quality of the microchannels formed after the first and second laser passes are examined using scanning electron microscopy and atomic force microscopy. The observation results show that the second laser pass yields an effective reduction in the surface roughness. The practicality of the proposed approach is demonstrated by fabricating a microfluidic chip for formaldehyde concentration detection. It is shown that the detection results obtained for five Chinese herbs with formaldehyde concentrations ranging from 5 to 55 ppm deviate by no more than 5.5 % from those obtained using a commercial macroscale device. In other words, the results confirm that the proposed defocused ablation technique represents a viable solution for the rapid and low-cost fabrication of a wide variety of glass-based microfluidic chips.

L.-M. Fu
Graduate Institute of Materials Engineering,
National Pingtung University of Science and Technology,
Pingtung 912, Taiwan
e-mail: loudyfu@mail.npust.edu.tw

W.-J. Ju · R.-J. Yang (✉)
Department of Engineering Science,
National Cheng Kung University, Tainan 70101, Taiwan
e-mail: rjyang@mail.ncku.edu.tw

Y.-N. Wang (✉)
Department of Vehicle Engineering, National Pingtung
University of Science and Technology, Pingtung 912, Taiwan
e-mail: yanwang@mail.npust.edu.tw

Keywords Defocused laser beam · CO_2 laser · Microfluidic chip · Formaldehyde

1 Introduction

The emergence of micro-electro-mechanical systems technologies in recent decades has prompted the development of many microfluidic devices for use in the biochemical, biomedical, food and environmental monitoring fields (Weng et al. 2009; Wang and Kang 2010; Smith et al. 2010; Chiavaroli et al. 2010; Koklu et al. 2010; Jiang et al. 2011; Wang et al. 2011a; Dong et al. 2011; Lee et al. 2011a; Lee et al. 2012a, b; Liao et al. 2012). Microfluidic devices have many advantages compared to their macroscale counterparts, including a reduced reaction solution and cell consumption, an improved analysis speed, a greater portability, a greater sensitivity, lower fabrication and operating costs, and the potential for parallel processing and integration with other miniaturized devices. Many researchers have demonstrated the feasibility of utilizing micromachining techniques to fabricate a network of microchannels on quartz, glass or polymer (PMMA, PDMS, PC) substrates (Lin et al. 2009; Zhao et al. 2011; Lia and Kim 2011; Luo et al. 2011; Gui et al. 2011; Lim and Lam 2012; Tsai et al. 2012) for such diverse applications as sample handling and pretreatment, species mixing, cell sorting and counting, DNA amplification, cell analysis and so forth (Lin et al. 2007, 2008; Fu and Lin 2007; Tsai et al. 2008; Wen et al. 2011; Islam et al. 2011; Kennedy et al. 2011; Li et al. 2011; Lee et al. 2011b; Chen et al. 2011; Nerguizian et al. 2012).

For microfluidic chips based on glass substrates, the microchannels are generally fabricated using a chemical etching method. However, chemical etching is impractical

Published online: 05 October 2012

for prototyping applications since it requires the use of a clean room environment and generates toxic by-products, which can only be safely disposed of following an expensive treatment process. As a result, the feasibility of laser processing as a means of patterning glass substrates has attracted significant attention in recent years.

Laser ablation provides a rapid and convenient means of patterning glass substrates and requires the use of neither a mask nor a mold (Chantal and Khan 2006; Waldbaur et al. 2011). When using an excimer laser to perform the patterning process, the glass is removed under the effects of a photochemical mechanism. Specifically, the photon energy within the laser beam is absorbed by the substrate and results in a breaking of the bonds between the glass molecules. (Note that a similar mechanism is responsible for the ablation process in the femtosecond laser processing technique. However, in this case, the photochemical mechanism involves both a multi-photon phenomenon and an electron avalanche effect.) However, conventional laser processing techniques have a number of drawbacks; including a poor transparency of the patterned channels and the risk of thermal distortion (Yen et al. 2006).

Various researchers have demonstrated the use of CO_2 laser systems in patterning and modifying polymer or glass-based devices (Yeh et al. 2010; Hou et al. 2011; Chung and Lin 2011; Lee et al. 2012a, b; Ju et al. 2012a; Li et al. 2012; Riahi 2012). For example, Chung et al. (2005) presented a novel method for eliminating the bulges on the rim of a micromachined channel on a PMMA substrate by coating the top surface of the substrate with a thin layer of PDMS or unexposed JSR photoresist prior to the ablation process. Nguyen and Huang (2006) utilized a commercial CO_2 laser system to fabricate a micromixer incorporating four patterned polymeric sheets. Similarly, Yang et al. (2007) used a CO_2 laser system to fabricate a PMMA-based microfluidic device for the encapsulation of ampicillin in chitosan microparticles. Nayak et al. (2009) investigated the effects of CO_2 laser power and scanning speed on the depth, width and surface profiles of microchannels patterned on PMMA substrates with various molecular weights. In general, the results showed that for all the considered substrates, the channel depth (and to a lesser extent, the channel width) increased with an increasing laser power or a reducing scanning speed. Yuan and Das (2007) performed an experimental and theoretical investigation into the micromachining of PMMA substrates using a CO_2 laser system. The results showed that microchannels with widths ranging from 44 to 240 μm and depths ranging from 22 to 130 μm could be obtained using a laser power of 0.45–1.35 W and a scanning speed of 2–14 mm/s. Chung et al. (2010) investigated the cracks formed during the through-wafer deep etching of Pyrex 7440 and medical-grade glass slides using a water-assisted CO_2 laser ablation method. Hong et al. (2010) fabricated an integrated microfluidic chip for methanol detection purposes using a novel continuous wave defocused CO_2 laser beam method. It was shown that the use of a defocused laser beam resulted in a significant reduction in the surface roughness compared to that obtained using a focused beam.

The use of UV, excimer laser and femtosecond laser micromachining techniques to pattern polymer- or glass-based devices has been widely reported (Edwards et al. 2011; Wang et al. 2011b; Conlisk et al. 2011; Svoboda et al. 2010). For example, Qi et al. (2008) fabricated a PMMA microfluidic biochip in which the substrate was patterned using an excimer laser with a central wavelength of 248 nm. Farson et al. (2008) used a femtosecond laser system to ablate microfluidic channels on soda-lime glass and fused quartz substrates. It was shown that by coating the substrate with a thin HEMA layer prior to the patterning process, the surface roughness of the ablated channel could be reduced to around 10 nm, irrespective of the original surface roughness condition. Iosin et al. (2011) proposed a new method for patterning PDMS microfluidic channels by means of a photocrosslinking mechanism mediated by a two-photon absorption process at the focal point of either a sub-nanosecond Nd:YAG microlaser or a femtosecond Ti:Sapphire laser. Ju et al. (2012b) patterned a glass substrate using a defocused femtosecond laser system and showed that the mean surface roughness of the ablated microchannel could be reduced to the order of approximately 5 nm by annealing the patterned substrate in a sintering oven at 650 °C for 5 h.

The present study proposes a rapid and low-cost method for the prototyping of glass-based microfluidic chips. The cost of the CO_2 laser system is ten times less expensive than the cost of the excimer laser, the femtosecond laser and wet etching equipments. In addition, the microfluidic chip machining process can be accomplished within minutes. In the proposed approach, the substrate is placed on a hotplate and the required microchannel configuration is then patterned using a two-pass defocused CO_2 laser beam technique. The surface roughness characteristics of the ablated microchannels are observed after each laser pass using scanning electron microscopy (SEM) and atomic force microscopy (AFM). The average surface roughness is more than 400 Å by the process of conventional focused laser beam ablation. The roughness can be reduced to be 25 Å by our two passes of the defocused laser beam treatment. In addition, the glass substrate is crack free. The feasibility of the proposed approach is demonstrated by manufacturing a glass-based microfluidic chip for formaldehyde concentration detection and then comparing the detection results obtained for five Chinese herbs with those obtained using a conventional macroscale system.

2 Experimental

To minimize the risk of cracking during the laser ablation process, the glass slides (Borofloat@ 33, Schott Technical Glass Solutions) were annealed at a temperature of 560 °C for 4 h in order to relieve any internal residual stress. In practice, the presence of contaminants such as particles, grease or organic matter on the substrate surface results in a significant reduction in the surface quality of the ablated microchannels. Thus, the substrates were cleaned in a mixture of H_2SO_4 and H_2O_2 (H_2SO_4: H_2O_2 = 3:1) and then rinsed in copious amounts of de-ionized (DI) water. The substrates were blown dry with nitrogen gas and were then baked on a hotplate at 100 °C for 5 min to remove any residual water molecules. Finally, the substrates were allowed to cool naturally to room temperature.

Figure 1 presents a schematic illustration of the experimental system used to pattern the glass substrates. The CO_2 laser (M-40, Laser Pro Venus laser system, Taiwan) had a maximum output power of 40 W, an output beam diameter of 3.5 mm, a focus spot diameter of 0.12 mm, a beam divergence (full angle) of 4 mrad and a wavelength of 10.6 μm. The beam scanning speed was programmable over the range of 0.5–100 cm/s. As shown in Fig. 1, the laser system was mounted on an 800 × 570 mm^2 *X–Y* platform driven by a DC servo control system. Furthermore, the substrate was placed on a hotplate maintained at a temperature of 310 °C to minimize the risk of cracking during the ablation process and to improve the surface quality of the ablated channel. The microchannel configuration was designed using a commercial software (CorelDraw) and was then converted into the control signals required to drive the *X–Y* platform in such a way as to reproduce the pattern on the substrate surface. Preliminary scribing tests were performed using two laser beam modes, namely a focused mode and a defocused mode. (Note that full details of the laser system, defocused ablation process and adhesive bonding technique used to assemble the microfluidic chip are available in a previous study by the current group (Hong et al. 2010).) Following each ablation process, the surface quality of the resulting microchannel was examined using a scanning electron microscope (SEM, Hitachi S-3000N, Japan) and an atomic force microscope (AFM, Veeco CP series, USA).

3 Results and discussions

3.1 Laser scribing of microchannels

When scribing microchannels using the focused beam method, the spot size is smaller and tends not to overlap as the laser beam is scanned over the substrate surface. As a result, distinct ripples are formed on the ablated surface and the surface roughness is correspondingly increased (Hong et al. 2010). By contrast, in the defocused beam method, the spot size is larger, and thus the ablated regions overlap as the laser beam is scanned. Consequently, the ripple effect is reduced and a smoother ablated surface is obtained.

Figure 2 presents SEM images of the microchannels fabricated using various scanning speeds (*V*) and defocused heights (λ). Note that in every case, the laser power (*P*) is equal to 12 W and the substrate is maintained at a temperature (*T*) of 310 °C. Figure 2a shows a microchannel fabricated using a single pass of the defocused laser beam with a defocused height of $\lambda_1 = 0.5$ mm and a scanning speed of $v_1 = 10$ cm/s. Previous studies have shown that the defocused laser beam method results in a lower roughness of the ablated surface than that obtained using a focused laser beam (Hong et al. 2010). However, the energy density within the direct-writing ablation region is still very large. Therefore, as shown in Fig. 2a, the surface of the ablated channel has a rough appearance and contains multiple adhered particles. To improve the quality of the ablated microchannel, a series of scribing trials were

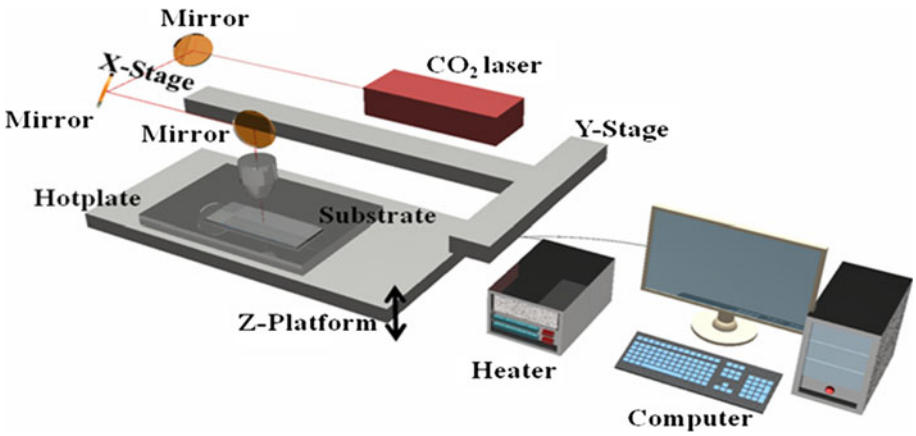

Fig. 1 Schematic illustration of CO_2 laser ablation system used to pattern glass substrates

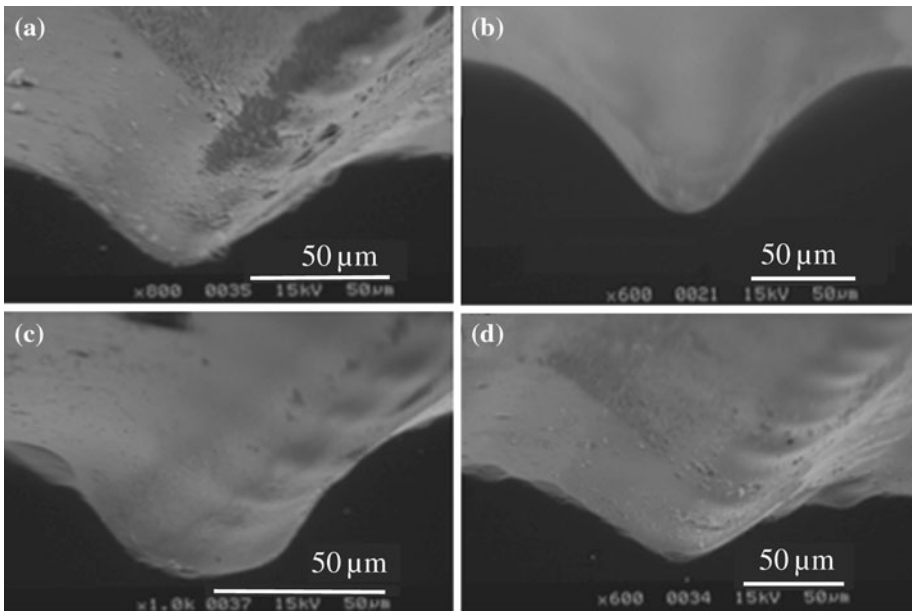

Fig. 2 SEM images of glass microchannels patterned using one or two defocused laser beam passes. **a** One laser beam pass with defocus height of 0.5 mm and scanning speed of 10 cm/s; **b** two laser beam passes with defocus height of 0.5 mm and scanning speed of 10 cm/s in the first pass, and 0.5 mm and 20 cm/s in the second pass; **c** two laser beam passes with defocus height of 0.5 mm and scanning speed of 10 cm/s in the first pass, and 1.0 mm and 20 cm/s in the second pass; **d** two laser beam passes with defocus height of 0.5 mm and scanning speed of 10 cm/s in the first pass, and 2.0 mm and 20 cm/s in the second pass. (Note that the scale bar is 50 µm, and the scanning power and hotplate temperature are equal to 12 W and 310 °C, respectively, in every case.)

performed in which the initial pass of the defocused laser beam (performed using the parameters described above) was followed by a second pass performed with a higher scanning speed of 20 cm/s and a defocused height of $\lambda_2 = 0.5$ mm (Fig. 2b), 1.0 mm (Fig. 2c) or 2.0 mm (Fig. 2d). Figure 2b shows that the surface roughness and number of adhered particles are both significantly reduced when the second laser pass is performed using the same defocused height as that used in the initial pass ($\lambda_1 = \lambda_2 = 0.5$ mm). Given a larger defocused height (i.e., $\lambda_2 = 1$ mm or 2 mm), the spot size increases and the energy intensity decreases. Thus, as shown in Fig. 2c, d, no significant improvement is obtained in the surface quality compared to that obtained using a single pass of the laser beam. It should be noted that the lower scanning speed will cause the heat accumulation and possible cracking on the substrate under high power machining process.

Figure 3a, b presents the AFM analyses of the surface roughness of the two microchannels fabricated by a single pass of the focused laser beam ($\lambda_1 = 0$ mm, $P_1 = 12$ W, $v_1 = 10$ cm/s, $T = 310$ °C) and two passes of the defocused CO_2 laser beam ($\lambda_1 = \lambda_2 = 0.5$ mm, $P_1 = P_2 = 12$ W, $v_1 = 10$ cm/s, $v_2 = 20$ cm/s, $T = 310$ °C), respectively. Note that the AFM analysis area is equal to 1×1 µm in both cases. It is seen that the use of the focused laser beam results in an average surface roughness of more than 400 Å. By contrast, the average surface roughness given two passes of the defocused laser beam is less than 25 Å. (Note that the average surface roughness was computed over five measurements taken at different positions on the ablated surface. Note further that the variance of the five measurements was less than 8 %.) The results presented in Fig. 3b confirm the effectiveness of the proposed two-pass defocused CO_2 laser beam method in fabricating microchannels with a surface roughness compatible with the requirements of glass-based microfluidic devices, i.e., <100 Å.

Figure 4 presents SEM images of three microchannels fabricated using the two-pass defocused laser beam method with processing parameters of $\lambda_1 = \lambda_2 = 0.5$ mm; $v_1 = 10$ cm/s; $v_2 = 20$ cm/s; $T = 310$ °C; $P_2 = 12$ W; and $P_1 =$ (a) 12 W, (b) 16 W, and (c) 20 W, respectively. It is seen that all three microchannels have a smooth appearance and contain no adhered particles. From inspection, the aspect ratios of the three channels are found to be 0.9, 1.1 and 1.3, respectively. In other words, the aspect ratio increases as the power used in the first laser pass increases. Overall, the results presented in Fig. 4 suggest that by applying a suitable laser power in the first ablation pass, a microchannel with the desired aspect ratio can be obtained, while by applying an equal (or lower) laser power in the second laser pass, the surface roughness of the ablated channel can be improved with no further change in the aspect ratio.

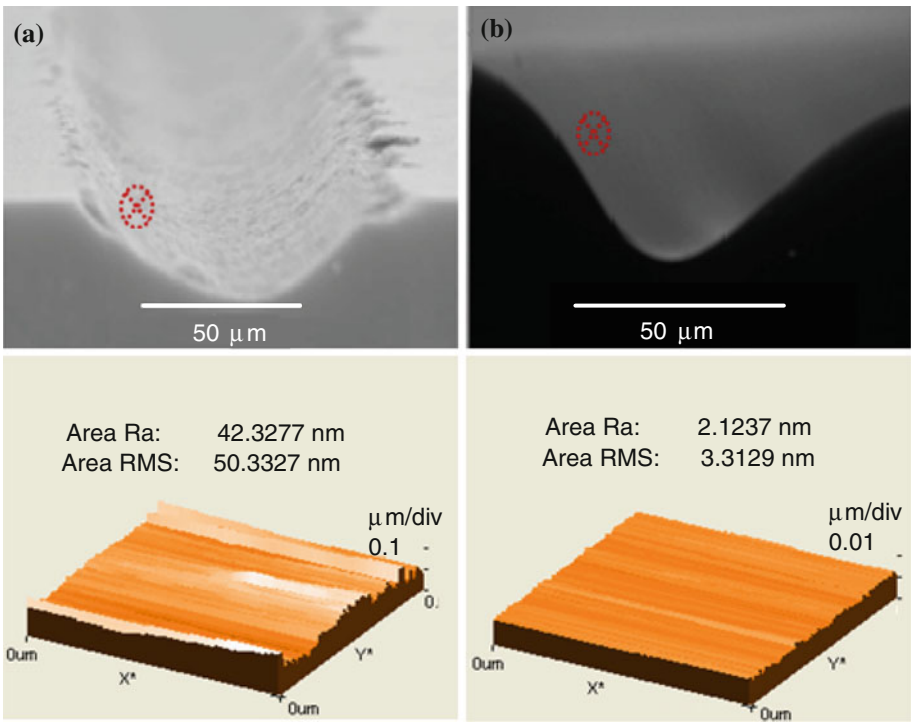

Fig. 3 AFM scanning results showing surface roughness of microchannels produced using: **a** single pass of defocused laser beam ($\lambda_1 = 0$ mm, $P_1 = 12$ W, $v_1 = 10$ cm/s, $T = 310$ °C) and **b** two passes of the defocused laser beam ($\lambda_1 = \lambda_2 = 0.5$ mm, $P_1 = P_2 = 12$ W, $v_1 = 10$ cm/s, $v_2 = 20$ cm/s, $T = 310$ °C)

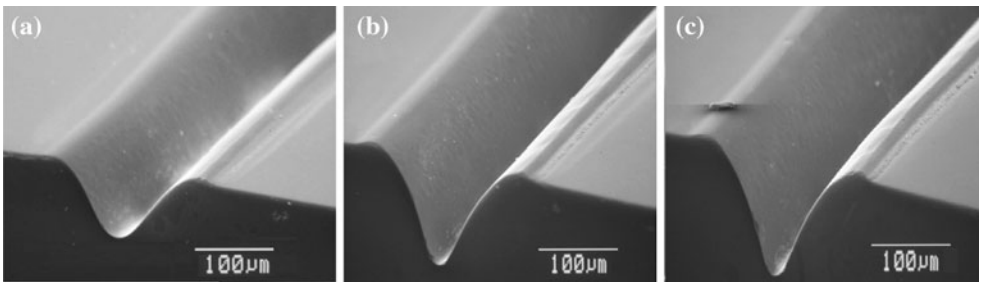

Fig. 4 SEM images of glass substrates containing three microchannels produced using two passes of defocused laser beam with different laser powers in the first pass, i.e., **a** $P_1 = 12$ W, **b** $P_1 = 16$ W and **c** $P_1 = 20$ W (Note that for all three images, $\lambda_1 = \lambda_2 = 0.5$ mm, $v_1 = 10$ cm/s, $v_2 = 20$ cm/s, $T = 310$ °C and $P_2 = 12$ W)

3.2 Fabrication of microfluidic chip using two-pass defocused laser beam method

Figure 5 presents a photograph of the formaldehyde detection microchip fabricated in the present study. Note that the microchannel network was fabricated using the following parameter settings: $P_1 = 16$ W, $v_1 = 10$ cm/s, $\lambda_1 = 0.5$ mm, $P_2 = 12$ W, $v_2 = 20$ cm/s, $\lambda_2 = 0.5$ mm, and $T = 310$ °C. As shown, the microchip incorporates two inlets for the formaldehyde sample and fuchsin reagent, a circular mixing chamber, a serpentine reaction chamber and a collection chamber, respectively.

Figure 6 illustrates the major steps involved in fabricating the microfluidic chip and performing the formaldehyde concentration detection process. The following

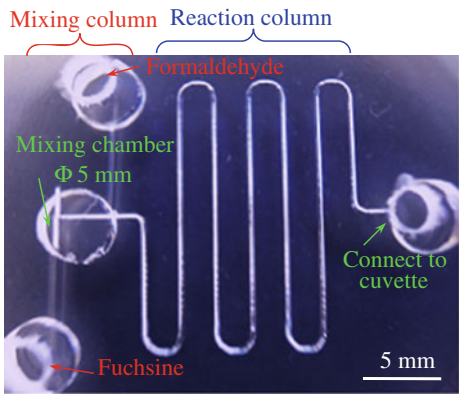

Fig. 5 Photograph of CO_2 laser-ablated microchip for formaldehyde concentration detection

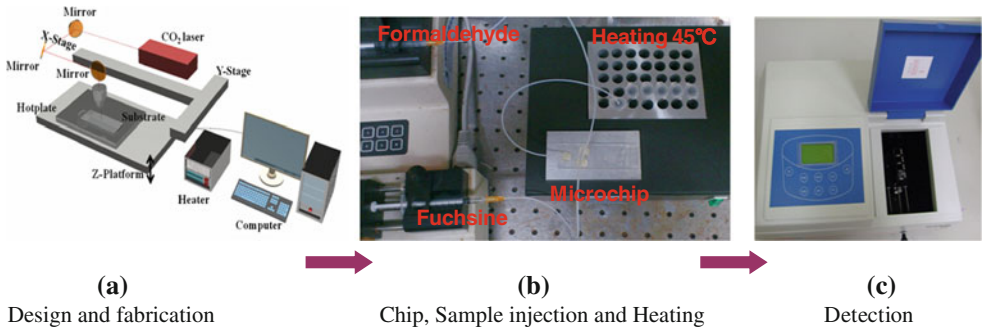

Fig. 6 Schematic illustration showing major steps in chip fabrication and formaldehyde concentration detection procedures

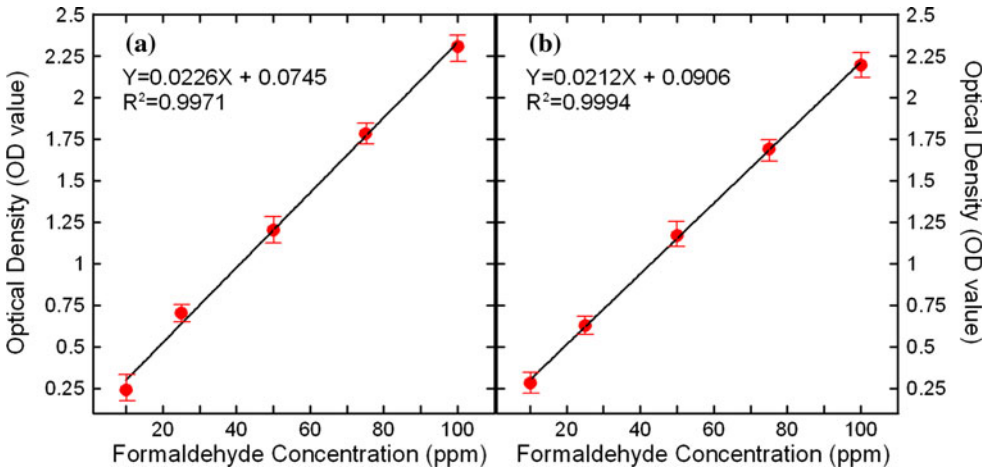

Fig. 7 Variation of optical density with formaldehyde concentration in: **a** conventional tube system and **b** CO_2 laser-ablated microchip

samples and reagent were prepared: (1) formaldehyde with concentrations ranging from 5 to 100 ppm, prepared by mixing formaldehyde and DI water in appropriate quantities; and (2) 200 µl of basic fuchsin ($C_{20}H_{19}N_3{\cdot}HCl$). As shown in Fig. 6b, the formaldehyde sample (800 µl, 28 ml/h) and fuchsin reagent (200 µl, 7 ml/h) were injected into the formaldehyde microchip by syringe pumps (KDS 100, USA) and mixed within the circular mixing chamber for 5 min before passing through the serpentine reaction column and entering the collection chamber. The mixture was then allowed to flow into a cuvette through a Teflon tube and heated at a constant temperature of 45 °C for approximately 15 min in order to prompt a colorimetric reaction. Finally, the cuvette was inserted into the detection trough of a UV spectrophotometer (UV-6100, Great Tide Instrument Co., Ltd) in order to analyze the absorbance spectrum (see Fig. 6c).

Figure 7a presents the results obtained using a conventional macroscale detection method for the variation of the optical density (OD) with the formaldehyde concentration for samples with known formaldehyde concentrations in the range of 10–100 ppm. (Note that the OD results represent the average value of five different measurements for each sample.) Applying a regression analysis technique to

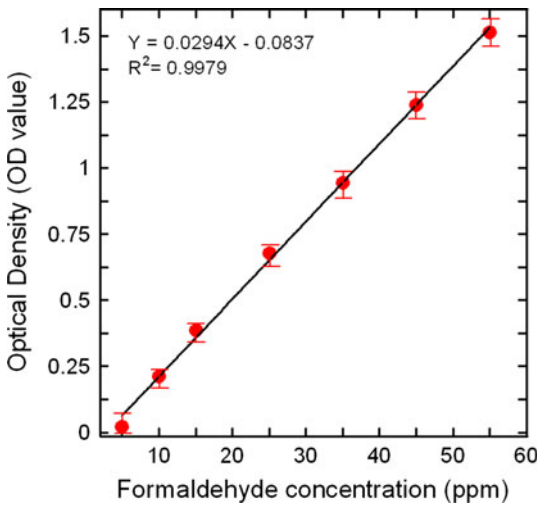

Fig. 8 Variation of optical density with formaldehyde concentration for samples with formaldehyde concentrations ranging from 5 to 55 ppm. (Note that the results represent the average values obtained over five separate measurements of each sample.)

the experimental data, it is found that the OD value (Y) and the formaldehyde concentration (X) are related as follows: $Y = 0.0226X + 0.0745$. Moreover, the correlation coefficient is found to be $R^2 = 0.9971$. Figure 7b illustrates the

Table 1 Formaldehyde concentration results obtained for five commercial Chinese herbs using CO_2 laser-ablated microfluidic chip and traditional macroscale detection system, respectively

Samples	Average OD value	Microfluidic chip (ppm)	NPUST CAAPIC detection (ppm)
Ginseng (solid)	0.1544	8.12	7.7
Dry mushroom	0.8483	31.71	31.3
Korean ginseng tea	0.0011	N.D.	N.D.
Dry Chinese yam	0.0025	N.D.	N.D.
Dry lotus seed	0.0017	N.D.	N.D.

Note that the average OD data relate to the microfluidic method and represent the average values obtained over five measurements of the corresponding sample

NPUST National Pingtung University Science Technology

CAAPIC Center for Agriculture and Aquaculture Product Inspection and Certification

N.D. Non-detectable

corresponding detection results obtained using the CO_2 laser-ablated microchip. From inspection, the OD value and the formaldehyde concentration are related via the relationship $Y = 0.0212X + 0.0906$. Moreover, the correlation coefficient has a value of $R^2 = 0.9994$. It is noted that the correlation coefficient is higher than that of the traditional macroscale method. Moreover, the detection limit is less than 2 ppm. In other words, the precision of the microfluidic formaldehyde detection chip is confirmed.

3.3 Formaldehyde detection in commercial Chinese herb samples

The suitability of the formaldehyde detection microchip for real-world applications was investigated using five commercial Chinese herbs samples with formaldehyde concentrations ranging from 5 to 55 ppm, namely Sample #1 (ginseng, solid, source: northeast China, Grocer, China); Sample #2 (dry mushroom, solid, Shenzhen Yongliansheng Industrial Trading Co., China); Sample #3 (Korean ginseng tea, powder, Kai Cheng Ginseng Enterprises Ltd., Taiwan); Sample #4 (dry Chinese yam, solid, Pang Chien Tang Co., China); and Sample #5 (dry lotus seed, solid, 007 Grocer Co., Taiwan). Figure 8 presents the corresponding detection results. From inspection, the optical density and formaldehyde concentration are found to be related via the relationship $Y = 0.0294\ \mathrm{X} - 0.0837$. Moreover, the correlation coefficient is found to have a value of $R^2 = 0.9979$. For reference purposes, the formaldehyde concentrations of the five samples were also measured by the Center for Agriculture and Aquaculture Product Inspection and Certification (CAAPIC, ISO/IEC 17025 Accreditation by Taiwan Accreditation Foundation) at National Pingtung University of Science and Technology (NPUST) in Taiwan using a traditional colorimetric method. The detection results obtained for the five samples using the two methods are summarized in Table 1. Note that the data in the average OD column relate to the microfluidic detection method and indicate the average OD value obtained over five separate measurements. Substituting the five average OD values into the regressional relationship shown in Fig. 8 (i.e., $Y = 0.0294X - 0.0837$), the corresponding formaldehyde concentrations are found to be 8.12 ppm for Sample #1, 31.71 ppm for Sample #2 and non-detectable for the remaining three samples. According to the results obtained from CAAPIC, the five samples have formaldehyde concentrations of 7.7 ppm for Sample #1, 31.1 ppm for Sample #2 and non-detectable for Samples #3 $\sim$ #5. Taking the results obtained from CAAPIC as reference values, the accuracy of the measurement results obtained using the microfluidic detection chip is found to be 94.5 % for Sample #1 and 98.0 % for Sample #2. (Note that the accuracy (%) is computed as $\text{Accuracy}\ (\%) = \left(1 - \left|\frac{\text{microfluidic method} - \text{macroscale method}}{\text{macroscale method}}\right|\right) \times 100\ \%$.) In other words, the applicability of the proposed microchip to the formaldehyde concentration measurement of real-world samples is confirmed.

4 Conclusions

This paper has presented a novel two-pass defocused CO_2 laser beam method for scribing microchannels in glass-based substrates. In the proposed approach, a hotplate is used to maintain the glass substrate at an appropriate temperature to minimize the risk of cracking and to improve the channel surface quality during the ablation process. The processing parameters used in the first pass are specified in such a way as to fabricate a microchannel with the required aspect ratio, while in the second pass, the processing parameters (power and scanning rate) are adjusted in such a way as to minimize the surface roughness without causing any further change in the aspect ratio. The SEM and AFM observation results have shown that a

microchannel surface roughness of less than 25 Å can be obtained by maintaining the substrate at a temperature of 310 °C and specifying the two-pass processing parameters as follows: laser power $P_1 = P_2 = 12$ W; defocused height $\lambda_1 = \lambda_2 = 0.5$ mm; scanning speed in first pass $v_1 = 10$ cm/s; and scanning speed in second pass $v_2 = 20$ cm/s. The practicality of the proposed defocused CO_2 laser beam method has been demonstrated by fabricating a microfluidic chip for formaldehyde concentration detection. The experimental results obtained for control samples with known formaldehyde concentrations of $10 \sim 100$ ppm have shown that the device has a high measurement linearity (i.e., a correlation coefficient of $R^2 = 0.9994$). Moreover, it has been shown that the detection results obtained by the proposed device for five commercial Chinese herbs with formaldehyde concentrations ranging from 5 to 55 ppm deviate by no more than 5.5 % from the measurement results obtained using a conventional macroscale system. Overall, the results confirm that the two-pass defocused CO_2 laser beam method presented in this study provides a low-cost and effective solution for the rapid prototyping of glass-based microfluidic devices.

Acknowledgments The authors gratefully acknowledge the financial support provided to this study by the National Science Council of Taiwan.

References

Chantal G, Khan M (2006) Laser processing for bio-microfluidics applications (Part I). Anal Bioanal Chem 385:1351–1361

Chen L, Algar WR, Tavares AJ, Krull UJ (2011) Toward a solid-phase nucleic acid hybridization assay within microfluidic channels using immobilized quantum dots as donors in fluorescence resonance energy transfer. Anal Bioanal Chem 399:133–141

Chiavaroli S, Newport D, Woulfe B (2010) An optical counting technique with vertical hydrodynamic focusing for biological cells. Biomicrofluidics 4:024110

Chung CK, Lin SL (2011) On the fabrication of minimizing bulges and reducing the feature dimensions of microchannels using novel CO_2 laser micromachining. J Micromech Microeng 21:065023

Chung CK, Lin YC, Huang GR (2005) Bulge formation and improvement of the polymer in CO_2 laser micromachining. J Micromech Microeng 15:1878–1884

Chung CK, Chang HC, Shih TR, Lin SL, Hsiao EJ, Chen YS, Chang EC, Chen CC, Lin CC (2010) Water-assisted CO_2 laser ablated glass and modified thermal bonding for capillary-driven biofluidic application. Biomed Microdevices 12:107–114

Conlisk K, Favre S, Lasser T, O'Connor GM (2011) Application of reconfigurable pinhole mask with excimer laser to fabricate microfluidic components. Microfluid Nanofluid 11:1247–1256

Dong T, Yang Z, Su Q, Tran NM, Egeland EB, Karlsen F, Zhang Y, Kapiris MJ, Jakobsen H (2011) Integratable non-clogging microconcentrator based on counter-flow principle for continuous enrichment of CaSki cells sample. Microfluid Nanofluid 10:855–865

Edwards TL, Harper JC, Polsky R, Lopez DM, Wheeler DR, Allen AC, Brozik SM (2011) A parallel microfluidic channel fixture fabricated using laser ablated plastic laminates for electrochemical and chemiluminescent biodetection of DNA. Biomicrofluidics 5:044115

Farson DF, Choi HW, Zimmerman B, Steach JK, Chalmers JJ, Olesik SV, Lee LJ (2008) Femtosecond laser micromachining of dielectric materials for biomedical applications. J Micromech Microeng 18:035020

Fu LM, Lin CH (2007) A rapid DNA digestion system. Biomed Microdevices 9:277–286

Gui L, Yu BY, Ren CL, Huissoon JP (2011) Microfluidic phase change valve with a two-level cooling/heating system. Microfluid Nanofluid 10:435–445

Hong TF, Ju WJ, Wu MC, Tai CH, Tsai CH, Fu LM (2010) Rapid prototyping of PMMA microfluidic chips utilizing a CO_2 laser. Microfluid Nanofluid 9:1125–1133

Hou HH, Wang YN, Chang CL, Fu LM, Yang RJ (2011) Rapid glucose concentration detection utilizing disposable integrated microfluidic chip. Microfluid Nanofluid 11:479–487

Iosin M, Scheul T, Nizak C, Stephan O, Astilean S, Baldeck P (2011) Laser microstructuration of three-dimensional enzyme reactors in microfluidic channels. Microfluid Nanofluid 10:685–690

Islam MZ, McMullin JN, Tsui YY (2011) Rapid and cheap prototyping of a microfluidic cell sorter. Cytometry A79A: 361–367

Jiang H, Weng X, Li D (2011) Microfluidic whole-blood immunoassays. Microfluid Nanofluid 10:941–964

Ju WJ, Fu LM, Yang RJ, Lee CL (2012a) Distillation and detection of SO_2 using microfluidic chip. Lab Chip 12:622–626

Ju WJ, Hong TF, Yang RJ, Fu LM, Lee CY (2012b) Rapid fabrication of glass-based microfluidic chips utilizing a femtosecond laser. Adv Sci Lett 8:416–420

Kennedy MJ, Stelick SJ, Sayam LG, Yen A, Ericksond D, Batt CA (2011) Hydrodynamic optical alignment for microflow cytometry. Lab Chip 11:1138–1143

Koklu M, Park S, Pillai SD, Beskok A (2010) Negative dielectrophoretic capture of bacterial spores in food matrices. Biomicrofluidics 4:034107

Lee HC, Hou HH, Yang RJ, Lin CH, Fu LM (2011a) Microflow cytometer for three-dimensional focusing with sequence microweir structure. Microfluid Nanofluid 11:469–478

Lee CY, Chang CL, Wang YN, Fu LM (2011b) Microfluidic mixing: a review. Int J Mol Sci 12:3263–3287

Lee CY, Leong JC, Wang YN, Fu LM, Chen SJ (2012a) A ferrofluidic magnetic micropump for variable-flow-rate applications. Jap J Appl Phys 51:047201

Lee HB, Oh K, Yeo WH, Lee TR, Chang YS, Choi JB, Lee KH, Kramlich J, Riley JJ, JH Chung, Kim YJ (2012b) Enhanced bioreaction efficiency of a microfluidic mixer toward high-throughput and low-cost bioassays. Microfluid Nanofluid 12:143–156

Li J, Zhang M, Wang L, Li W, Sheng P, Wen W (2011) Design and fabrication of microfluidic mixer from carbonyl iron–PDMS composite membrane. Microfluid Nanofluid 10:919–925

Li M, Li S, Wu J, Wen W, Li W, Alici G (2012) A simple and cost-effective method for fabrication of integrated electronic-microfluidic devices using a laser-patterned PDMS layer. Microfluid Nanofluid 12:751–760

Lia M, Kim DP (2011) Silicate glass coated microchannels through a phase conversion process for glass-like electrokinetic performance. Lab Chip 11:1126–1131

Liao SH, Cheng IF, Chang HC (2012) Precisely sized separation of multiple particles based on the dielectrophoresis gradient in the z-direction. Microfluid Nanofluid 12:201–211

Lim CY, Lam YC (2012) Analysis on micro-mixing enhancement through a constriction under time periodic electroosmotic flow. Microfluid Nanofluid 12:127–141

Lin CH, Tsai CH, Pan CW, Fu LM (2007) Rapid circular microfluidic mixer utilizing unbalanced driving force. Biomed Microdevices 9:43–50

Lin CH, Wang JH, Fu LM (2008) Improving the separation efficiency of DNA biosamples in capillary electrophoresis microchips using high-voltage pulsed DC electric fields. Microfluid Nanofluid 5:403–410

Lin C, Lee C, Tsai C, Fu L (2009) Novel continuous particle sorting in microfluidic chip utilizing cascaded squeeze effect. Microfluid Nanofluid 7:499–508

Luo C, Xiang M, Liu X, Wang H (2011) Transition from Cassie–Baxter to Wenzel States on microline-formed PDMS surfaces induced by evaporation or pressing of water droplets. Microfluid Nanofluid 10:831–842

Nayak NC, Lam YC, Yue CY, Sinha AT (2009) CO_2-laser micromachining of PMMA: the effect of polymer molecular weight. J Micromech Microeng 18:095020

Nerguizian V, Alazzam A, Roman D, Stiharu I Jr, Burnier M (2012) Analytical solutions and validation of electric field and dielectrophoretic force in a bio-microfluidic channel. Electrophoresis 33:426–435

Nguyen NT, Huang X (2006) Modelling, fabrication and characterization of a polymeric micromixer based on sequential segmentation. Biomed Microdevices 8:133–139

Qi H, Chen T, Yao L, Zuo T (2008) Hydrophilicity modification of poly(methyl methacrylate) by excimer laser ablation and irradiation. Microfluid Nanofluid 5:139–143

Riahi M (2012) Fabrication of a passive 3D mixer using CO_2 laser ablation of PMMA and PDMS moldings. Microchem J 100:14–20

Smith RL, Demers CJ, Collins SD (2010) Microfluidic device for the combinatorial application and maintenance of dynamically imposed diffusional gradients. Microfluid Nanofluid 9:613–622

Svoboda M, Slouka Z, Schrott W, Červenka P, Přibyl M, Šnita D (2010) Fabrication of plastic microchips with gold microelectrodes using techniques of sacrificed substrate and thermally activated solvent bonding. Microelectron Eng 87:1590–1593

Tsai CH, Hou HH, Fu LM (2008) An optimal three-dimensional focusing technique for micro-flow cytometers. Microfluid Nanofluid 5:827–836

Tsai CH, Yeh CP, Lin CH, Yang RJ, Fu LM (2012) Formation of recirculation zones in a sudden expansion microchannel with a rectangular block structure over a wide Reynolds number range. Microfluid Nanofluid 12:213–220

Waldbaur A, Rapp H, Lange K, Rapp BE (2011) Let there be chip-towards rapid prototyping of microfluidic devices: one-step manufacturing processes. Anal Methods 3:2681–2716

Wang M, Kang Q (2010) Electrochemomechanical energy conversion efficiency in silica nanochannels. Microfluid Nanofluid 9:181–190

Wang J, Wang C, Lin C, Lei H, Lee G (2011a) An integrated microfluidic system for counting of $CD4^+$/$CD8^+$T lymphocytes. Microfluid Nanofluid 10:531–541

Wang ZK, Zheng HY, Xia HM (2011b) Femtosecond laser-induced modification of surface wettability of PMMA for fluid separation in microchannels. Microfluid Nanofluid 10:225–229

Wen CY, Liang GB, Chen H, Fu LM (2011) Numerical analysis of a rapid magnetic microfluidic mixer. Electrophoresis 32:3268–3279

Weng X, Chon CH, Jiang H, Li D (2009) Rapid detection of formaldehyde concentration in food on a polydimethylsiloxane (PDMS) microfluidic chip. Food Chem 114:1079–1082

Yang CH, Huang KS, Chang JY (2007) Manufacturing monodisperse chitosan microparticles containing ampicillin using a microchannel chip. Biomed Microdevices 9:253–259

Yeh CH, Lin PW, Lin YC (2010) Chitosan microfiber fabrication using a microfluidic chip and its application to cell cultures. Microfluid Nanofluid 8:115–121

Yen MH, Cheng JY, Wei CW, Chuang YC, Young TH (2006) Rapid cell-patterning and microfluidic chip fabrication by crack-free CO_2 laser ablation on glass. J Micromech Microeng 16:1143–1153

Yuan D, Das S (2007) Experimental and theoretical analysis of direct-write laser micromachining of polymethyl methacrylate by CO_2 laser ablation. J Appl Phys 101:024901

Zhao L, Li S, Hu H, Guo Z, Guo F, Zhang N, Ji X, Liu W, Liu K, Guo S, Zhao X (2011) A novel method for generation of amphiphilic PDMS particles by selective modification. Microfluid Nanofluid 10:453–458